Relativistic meson spectroscopy and in-medium effects

Alan J. Sommerer, A. Abd El-Hady, and John R. Spence Department of Physics and Astronomy, Iowa State University, Ames, IA 50011

and James P. Vary

Department of Physics and Astronomy, Iowa State University,

Ames, IA 50011 and

Institute for Theoretical Physics, University of Heidelberg,

D-69120 Heidelberg, Germany.

September 4, 2018

Abstract

We extend our earlier model of $q\bar{q}$ mesons using relativistic quasipotential (QP) wave equations to include open-flavor states and running quark-gluon coupling effects. Global fits to meson spectra are achieved with rms deviations from experiment of 43-50 MeV. We examine in-medium effects through their influence on the confining interaction and predict the confining strength at which the masses of certain mesons fall below the threshold of their dominant decay channel.

PACS numbers: 11.10.Qr, 11.10.St, 12.40.Qq

Interest in calculating the properties of hadronic matter has grown in recent years because it is believed that understanding the behavior of these properties in high density and temperature environments is necessary for interpreting the results of relativistic heavy ion collisions. It is expected that observables such as masses, widths, and couplings will change in hot, dense environments like those achieved in experiments attempting to create conditions for the phase transition to the quark-gluon plasma [1].

Several papers have treated constituent quark models using two-body relativistic wave equation treatments [2,3]. We here improve and extend the model of Ref. [3] by including open-flavor mesons in the spectrum fits and incorporating a running quark-gluon coupling. We then provide initial results for in-medium effects through their influence on the confining interaction.

The interaction kernel consists of a one-gluon exchange interaction in the ladder approximation, V_{OGE} , and a phenomenological, long-range confinement potential, V_{CON} . We treat the potentials in momentum-space according to the methods described in Ref. [4]. This interaction takes the form

$$V_{OGE} + V_{CON} = \frac{4}{3} \alpha_s \frac{\gamma_\mu \otimes \gamma_\mu}{(q - q')^2} + \sigma \lim_{\mu \to 0} \frac{\partial^2}{\partial \mu^2} \frac{\mathbf{1} \otimes \mathbf{1}}{-(q - q')^2 + \mu^2}.$$
 (1)

Here, α_s is the strong coupling, which is weighted by the meson color factor of $\frac{4}{3}$, and the string tension σ is the strength of the confining part of the interaction. We adopt a scalar Lorentz structure V_{CON} since this choice is supported by lattice results [5] and by phenomenology, e.g. [3].

There are several choices of relativistic two-body wave equations which can be used to treat the interactions of Eq. (1). In this investigation, we employ two different equations, a spinor version of the Thompson equation [6] and the equation introduced in Ref. [3]. For convenience, we will refer to these equations as "reduction A" and "reduction B" respectively. These two integral equations result from different choices of three-dimensional propagators used to reduce the Bethe-Salpeter equation from four to three dimensions.

Assuming a bound state of quarks with equal masses in the center-of-mass 0^- channel, the reduction A equation reads

$$(2\omega - E)\psi_{+}^{0}(q) = \frac{4\alpha_{s}}{3\pi q}I_{1}(q, q') + \frac{\sigma}{2\pi q}I_{2}(q, q'), \tag{2}$$

and the reduction B equation reads

$$(4\omega^2 - E^2)\,\psi_+^0(q) = \frac{8\alpha_s E}{3\pi q} I_1(q, q') + \frac{\sigma E}{\pi q} I_2(q, q'). \tag{3}$$

In each case

$$I_1(q, q') = \int_0^\infty dq' q' Q_0(Z) \frac{2\omega\omega' - m^2}{\omega\omega'} \psi_+^0(q'), \tag{4}$$

and

$$I_2(q,q') = \lim_{\mu \to 0} \frac{\partial^2}{\partial \mu^2} \int_0^\infty dq' q' \left\{ Q_0(Z') \frac{-\omega \omega' - m^2}{\omega \omega'} + \left[Z' Q_0(Z') - 1 \right] \frac{qq'}{\omega \omega'} \right\} \psi_+^0(q'). \tag{5}$$

The quantities q and q' are magnitudes of relative three-momenta, $\omega^{(')} = [m^2 + q^{(')2}]^{1/2}$, m is the constituent quark mass, Q_0 is the Legendre function of the second kind with argument $Z = (q^2 + q'^2)/2qq'$ or $Z' = (q^2 + q'^2 + \mu^2)/2qq'$, and E is the energy to be solved for along with the amplitudes ψ_+^0 . The '+' subscript on the amplitudes indicates that only the positive energy components have been retained in these equations.

We have improved the calculated spectra of Ref. [3] by incorporating a running strong coupling into the model. Specifically, we have constrained the coupling to run as in the leading log expression for α_s ,

$$\alpha_s(Q^2) = \frac{4\pi\alpha_s(\mu^2)}{4\pi + \beta_1\alpha_s(\mu^2)\ln(Q^2/\mu^2)},\tag{6}$$

where $\beta_1 = 11 - 2n_f/3$ and n_f is the number of quark flavors. The most precise measurements of α_s have been at M_Z , the mass of the Z-boson [7]: $\alpha_s(\mu^2 = M_Z^2) \simeq 0.12$, and the running couplings used in the following calculations are anchored to this point. We have elected to relate Q^2 to the meson mass scale through

$$Q^2 = \xi^2 M_{meson}^2 + \rho^2, (7)$$

where the parameters ξ and ρ are determined by the fit. The second term, if it is large enough, ensures a finite saturation value of α_s as Q^2 goes to zero.

We have also expanded the work of Ref. [3] by including open-flavor mesons in our fit.

The constituent masses, the string tension σ , and the parameters ξ and ρ are adjusted to minimize the RMS deviation between the calculated meson masses and the experimental masses listed in the Particle Data Tables [8].

There is the well debated issue of whether the low-mass pion (and later, when open-flavor states are considered, the K meson) should be included in a constituent quark model picture, even a relativistic one. We adopt the philosophy that if a model adequately reproduces the π and K masses, then these states may be retained in the calculations using that model. In the present case, reduction A does poorly at representing these low-mass mesons, and these states are therefore not included in calculations using reduction A.

The global fits includes 45 states for reduction A and 47 state for reduction B. The fitted parameters are given in Table 1. We list the complete calculated spectrum from both reductions in Table 2.

We turn now to a consideration of how this meson model may be used to treat in-medium effects on mesons. In-medium effects may be expected to modify primarily the long-range part of the interactions. We therefore focus our attention on the confining potential in this simple demonstration of the utility of our meson model. We use reduction B and the parameters from the global fit of Table 1 for these examples.

In order to make our calculations independent of a particular model for the medium effects on the string tension, and to avoid the necessity of invoking an equilibrium picture of the medium, we plot the meson masses against σ/σ_0 , where σ_0 is the vacuum value of the string tension. Given a model for the behavior of string tension with respect to a particular variable such as the temperature T, this plot of mass vs. σ/σ_0 can be converted into a plot of mass vs. temperature.

It is especially interesting to predict whether meson masses fall below thresholds resulting in the closing of decay channels and leading to significant modifications in meson widths. For this purpose we evaluate the masses of ψ'' and the D meson as a function of decreasing string tension and display the results in Figure 1.

The calculated ψ'' and D masses each differ from the measured masses by about 30 MeV.

In order to make the curves of Figure 1 pass exactly through the ψ'' and D (×2) measured masses for $\sigma/\sigma_0 = 1$, we plot $M(\sigma)M_{exp}/M(\sigma_0)$ on the vertical axis, where $M(\sigma)$ is the meson mass calculated using the in-medium string tension σ , and $M(\sigma_0)$ is the meson mass calculated using the vacuum value of the string tension σ_0 .

Figure 1 shows that the ψ'' mass crosses the $D\bar{D}$ threshold at a mass of about 3.71 GeV when the string tenion falls to about $0.9\sigma_0$. For string tensions less than this, the avenue for $\psi(3770)$ decay to $D\bar{D}$ is blocked. Since this is by far the dominant decay channel for the ψ'' in the vacuum [8], the model predicts significant modifications in its decay signatures will result when medium effects decrease the effective string tension by more than about 10%. A similar calculation using reduction A also shows this "cross over" at $\sigma = 0.9\sigma_0$.

In Figure 2 we show similar calculations for the masses of the ϕ and the $K\bar{K}$ threshold as a function of σ/σ_0 . The figure shows that the ϕ mass crosses the $K\bar{K}$ threshold at a mass of about 9.8 GeV when $\sigma/\sigma_0 \simeq 0.67$.

The results displayed in Figs. 1 and 2 may be interpreted within the framework of particular models of medium effects on the string tension. For example, several methods have been proposed for modeling the temperature dependence of the string tension [9-12] and they exhibit the common feature of predicting a monotonically decreasing string tension for increasing temperature.

According to a model for $\sigma(T)$ taken from Ref. [12], as a particular example,

$$\sigma(T)/\sigma(0) = \sqrt{1 - (T/T_c)^2},\tag{8}$$

where T_c is the critical temperature and T is the temperature of the medium. Applying this model to the $\psi'' - D\bar{D}$ plot in Figure 1, our calculation predicts that the ψ'' will cross the $D\bar{D}$ threshold at a temperature of 0.43 T_c .

We may compare our result of 0.43 T_c with the value of 0.56 T_c obtained in the study of Ref. [14] which also used Eq. (8) to model $\sigma(T)$. This difference may be attributed to the use of different constituent quark models. Ref. [14] used a non-relativistic Schrödinger equation treatment to compute the ψ'' mass, and a bag model to determine the location of the $D\bar{D}$ threshold by using scaling arguments to relate bag pressure to string tension. Our

model treats all states within a common relativistic framework.

Turning now to the $\phi - K\bar{K}$ system of Fig. 2, if we again use Eq. (8) to model the temperature dependence of the string tension, we observe that the $K\bar{K}$ decay channel of the ϕ will close at a temperature of about 0.74 T_c .

We may relate this result to that of a previous study [15] which used a Nambu-Jona-Lasinio model of in-medium ϕ and K masses. In this previous study, the $K\bar{K}$ decay channel for the ϕ was found to close at a temperature of

$$T \simeq 0.45 \ m_l, \tag{9}$$

where m_l is the value of the light constituent quark mass in a free hadron. Ref. [15] presents sample results for light-quark masses in the range 300 MeV $< m_l < 600$ MeV. Using the light constituent quark mass obtained in our spectrum fits, $m_l \simeq 340$ MeV (see Table 1), Eq. (9) predicts that the $K\bar{K}$ decay channel will become closed for ϕ decay at a temperature of about 150 MeV. We see that our result of 0.74 T_c would be comparable provided we assumed $T_c \simeq 200$ MeV.

Our relativistic in-medium calculations extend the work of previous non-relativistic potential models by providing a consistent relativistic framework for evaluating in-medium effects, through the dependence of our model parameters on properties of the medium. Work in-progress includes calculations of a large set of vacuum and in-medium observables for all meson states.

This work was supported in part by the U.S. Department of Energy under Grant No. DE-FG02-87ER40371, Division of High Energy and Nuclear Physics. JPV acknowledges support from the Alexander von Humboldt Foundation. We acknowledge valuable discussions with J. W. Qiu, S. P. Klevansky, R. Vogt, J. Hill, F. Wohn, and W. Weise.

References

- [1] See for example, J. D. Bjorken, Phys. Rev. **D27**, 140 (1983); Robert D. Pisarski and Frank Wilczek, Phys. Rev. **D29**, 338 (1984); Helmut Satz, "Color Screening and Quark Deconfinemet in Nuclear Collision", in *Quark-Gluon Plasma*, R. C. Hwa, ed., World Scientific, pp. 563-630 (1990); C. P. Singh, Phys. Rep. **236**, 147 (1993).
- See, for example, H. W. Crater and P. Van Alstine, Phys. Rev. D 37, 1982 (1988); F. Gross and J. Milana, Phys. Rev. D45, 969 (1992); P. C. Tiemeijer and J. A. Tjon, Phys. Lett. B277, 38 (1992); K. M. Maung, D. E. Kahana, and J. W. Norbury, Phys. Rev. D47, 1182 (1993); J. R. Spence and J. P. Vary, Phys. Rev. CC47, 1282 (1993).
- [3] A. J. Sommerer, J. R. Spence, and J. P. Vary, Mod. Phys. Lett. A 8, 3537 (1993); A.
 J. Sommerer, J. R. Spence, and J. P. Vary, Phys. Rev. C 49, 513 (1994).
- [4] D. Eyre and J. P. Vary, Phys. Rev. D 34, 3467 (1986); J. R. Spence and J. P. Vary, Phys. Rev. D 35, 2191 (1987).
- [5] E. Laermann, in Proceedings of Particles and Nuclei International Conference XIII (World Scientific, Singapore, in press); Y. Koike, Phys. Lett. B216, 84 (1989).
- [6] R. H. Thompson, Phys. Rev. D1, 110 (1970).
- [7] L3 Collaboration, Phys. Rep. **236**, 1 (1993).
- [8] Particle Data Group, Phys. Rev. D50 (1994).
- [9] F. Karsch, M. T. Mehr, and H. Satz, Z. Phys. C37, 617 (1988).
- [10] T. Hashimoto, O. Miyamura, K. Hirose, and T. Kanki, Phys. Rev. Lett. 57, 2123 (1986).
- [11] T. Takagi, Phys. Rev. D34, 1646 (1986).
- [12] R. D. Pisarski and O. Alvarez, Phys. Rev. D26, 3735 (1982).
- [13] M. Gao, Nucl. Phys. B (Proc. Suppl.) 9, 368 (1989).

- [14] R. Vogt and A. Jackson, Phys. Lett. **B206**, 333 (1988).
- [15] J. B. Blaizot and R. M. Galain, Phys. Lett. B271, 32 (1991).

Table 1.

Best values for the fitted parameters for reductions A, B. Best values for the seven parameters were determined by a fit to 45 (47) meson states for reduction A (B). "RMS" is the root-mean-squared deviation of the fitted meson masses from measured meson masses. Spectra are given in Table 2.

	A	В
$m_b \; (\mathrm{GeV})$	4.65	4.68
$m_c \; (\mathrm{GeV})$	1.37	1.39
$m_s \; ({\rm GeV})$	0.397	0.405
$m_u \; (\mathrm{GeV})$	0.339	0.346
$\sigma \; (\mathrm{GeV^2})$	0.233	0.211
ξ	0.616	0.444
$\rho \; (\text{GeV})$	0.198	0.187
RMS (MeV)	43	50

Table 2.

Fitted spectra for reductions A and B. The seven parameters used to obtain these spectra are given in Table 1.

Figure 1.

Plot of the ψ'' mass and the $D\bar{D}$ threshold as a function of σ/σ_0 , where σ is the in-medium value for the string tension and σ_0 is the vacuum value of the string tension. Masses were calculated with reduction B using the parameters of Table 1. Since using these parameters does not yield precisely the experimental vacuum values of the ψ'' and D masses, the vertical axis plots $M(\sigma)M_{exp}/M(\sigma_0)$ so that the curves pass exactly through the experimental masses at $\sigma/\sigma_0 = 1$.

Figure 2.

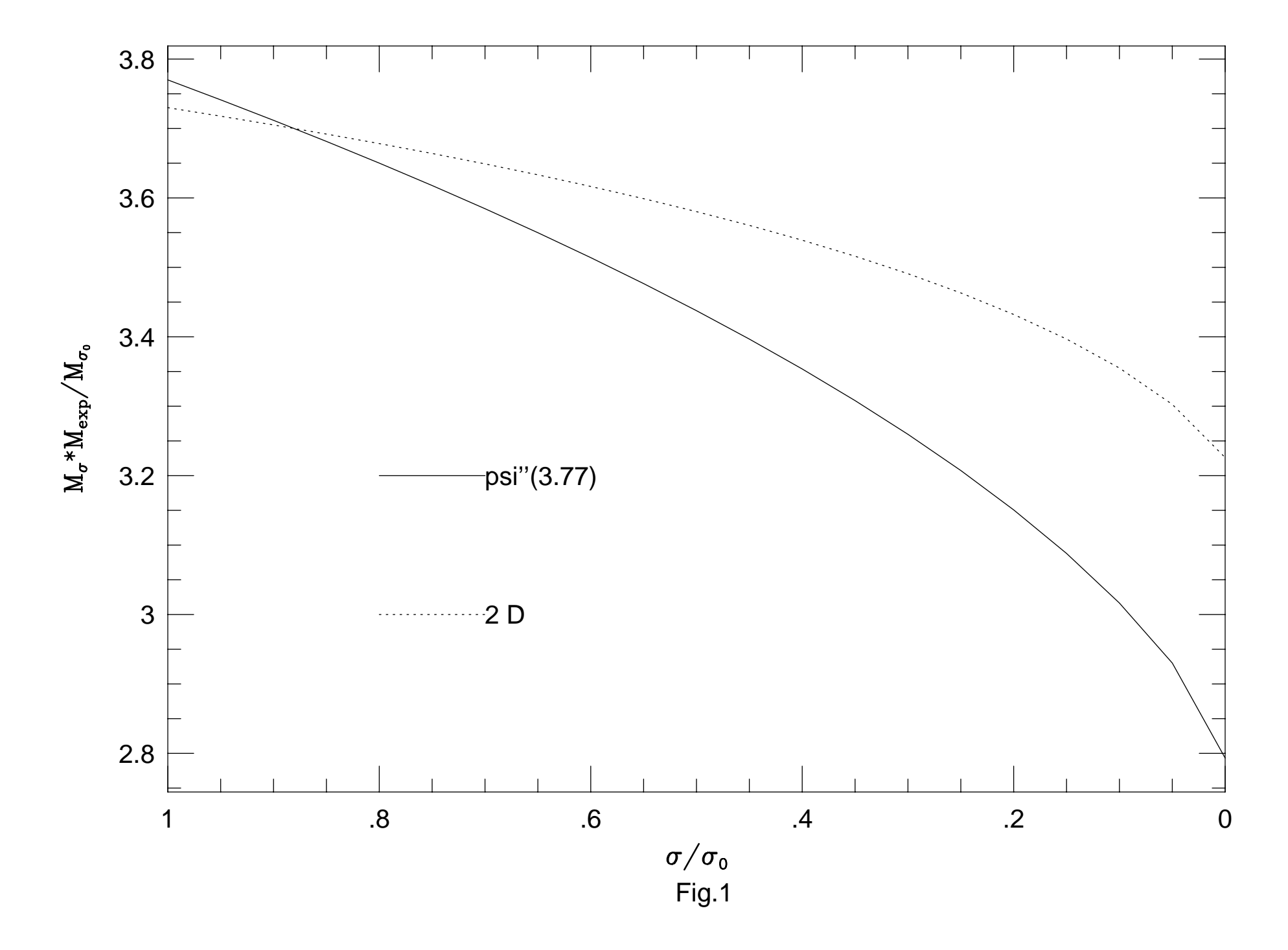
Plot of the ϕ mass and the $K\bar{K}$ threshold as a function of σ/σ_0 , where σ is the in-medium value for the string tension and σ_0 is the vacuum value of the string tension. Masses were calculated with reduction B using the parameters of Table 1. Since using these parameters does not yield precisely the experimental vacuum values of the ϕ and K masses, the vertical axis plots $M(\sigma)M_{exp}/M(\sigma_0)$ so that the curves pass exactly through the experimental values at $\sigma/\sigma_0 = 1$.

π	140	-	135
$\pi(1300)$	1300	1328	1439
π_2	1670	1536	1515
a_1	1260	1266	1223
b_1	1232	1262	1219
ρ	768	757	812
a_2	1318	1402	1367
ϕ	1019	1020	1020
$\overset{}{\phi}{}'$	1680	1678	1645
f_2'	1525	1558	1526
$\eta_c(1S)$	2979	2975	2993
$\eta_c(2S)$	3590	3624	3640
	3415	3402	3383
$\chi_{c0}(1P)$	3511	3486	
$\chi_{c1}(1P)$			3461
$h_c(1P)$	3526	3493	3471
$J/\psi(1S)$	3097	3113	3091
$\psi(2S)$	3686	3688	3688
$\psi(3770)$	3770	3760	3741
$\psi(4040)$	4040	4077	4104
$\psi(4160)$	4159	4122	4136
$\psi(4415)$	4415	4415	4456
$\chi_{c2}(1P)$	3556	3581	3556
$\chi_{b0}(1P)$	9860	9842	9843
$\chi_{b0}(2P)$	10232	10200	10198
$\chi_{b1}(1P)$	9892	9860	9863
$\chi_{b1}(2P)$	10255	10216	10214
$\Upsilon(1S)$	9460	9514	9520
$\Upsilon(2S)$	10023	9996	9996
$\Upsilon(3S)$	10355	10334	10331
$\Upsilon(4S)$	10580	10614	10611
$\Upsilon(10860)$	10865	10861	10860
$\Upsilon(11020)$	11019	11083	11086
$\chi_{b2}(1P)$	9913	9925	9928
$\chi_{b2}(2P)$	10268	10271	10270
K	494	-	495
$K_1(1406)$	1406	1360	1330
$K_1(1270)$	1270	1336	1287
K_2	1770	1631	1633
K^*	892	902	916
K_2^*	1426	1481	1442
D	1865	1852	1897
$D^*(2007)$	2007	2034	2004
$D^*(2420)$	2420	2397	2358
D_S	1971	1928	1968^{12}
D_S^*	2110	2108	2076
B°	5271	5322	5342
B^*	5352	5328	5347
	•	•	

Table 2.

This figure "fig1-1.png" is available in "png" format from:

http://arxiv.org/ps/nucl-th/9412029v1



This figure "fig1-2.png" is available in "png" format from:

http://arxiv.org/ps/nucl-th/9412029v1

